

Development of an *in vitro* mechanistic toxicity screening model using cultured hepatocytes

by Jacob John van Tonder

A thesis submitted in partial fulfilment of the requirements for the degree

Doctor of Philosophy in Pharmacology

in the
Faculty of Health Sciences
at the
University of Pretoria

Supervisor: Prof. V. Steenkamp

Co-supervisors: Dr. A.D. Cromarty

Prof. M. Gulumian

Pretoria November 2011

i



Declaration

University of Pretoria

Faculty of Health Sciences

Department of Pharmacology

I, Jacob John van Tonder,

Student number: 21038491

Subject of the work: Development of an in vitro mechanistic toxicity screening model using

cultured hepatocytes

Declaration

1. I understand what plagiarism entails and am aware of the University's policy in this regard.

2. I declare that this project (e.g. essay, report, project, assignment, dissertation, thesis etc.) is my own, original work. Where someone else's work was used (whether from a printed source, the internet or any other source) due acknowledgement was given and reference was made according to the departmental requirements.

3. I did not make use of another student's previous work and submitted it as my own.

4. I did not allow and will not allow anyone to copy my work with the intention of presenting it as his or her own work.

Signature:



Acknowledgments

- Prof. Vanessa Steenkamp and Dr. Duncan Cromarty for their guidance in the scientific process and taking the necessary steps to safeguard the quality of the results from this study. Teaching me the importance of objectivity and proving that my observations are accurate. For their patience and commitment.
- Prof. Mary Gulumian for her time and effort, ensuring that the interpretation of the results were accurate.
- Tracy Snyman, Clinical Chemistry at WITS, for her generous help regarding the propagation of the HepG2 cell line.
- Prof. Francois Steffens for pointing me in the right direction concerning statistical analyses and interpretation.
- My wife, Alet van Tonder, for her support, patience and understanding.
- God, for His faithfulness.

"Science is facts; just as houses are made of stones, so is science made of facts; but a pile of stones is not a house and a collection of facts is not necessarily science."

Henri Poincare



Abstract

In vitro testing includes both cell-based and cell-free systems that can be used to detect toxicity induced by xenobiotics. In vitro methods are especially useful in rapidly gathering intelligence regarding the toxicity of compounds for which none is available such as new chemical entities developed in the pharmaceutical industry. In addition to this, in vitro investigations are invaluable in providing information concerning mechanisms of toxicity of xenobiotics. This type of toxicity testing has gained popularity among the research and development community because of a number of advantages such as scalability to high throughput screening, cost-effectiveness and predictive power. Hepatotoxicity is one of the major causes of drug attrition and the high cost associated with drug development poses a heavy burden on the development of new chemical entities. Early detection of hepatotoxic agents by in vitro methods will improve lead optimisation and decrease the cost of drug development and reduce drug-induced liver injury. Literature highlights the need for a cell-based in vitro model that is capable of assessing multiple toxicity parameters, which assesses a wider scope of toxicity and would be able to detect subtle types of hepatotoxicity.

The present study was aimed at developing an *in vitro* procedure capable of mechanistically profiling the effects of known hepatotoxin dichlorodiphenyl trichloroethane (DDT) and its metabolites, dichlorodiphenyl dichloroethylene (DDE) and dichlorodiphenyl dichloroethane (DDD) on an established liver-derived cell line, HepG2, by evaluating several different aspects of cellular function using a number of simultaneous *in vitro* assays on a single 96 well microplate. Examined parameters have been suggested by the European Medicines Agency and include: cell viability, phase I metabolism, oxidative stress, mitochondrial toxicity and mode of cell death (apoptosis *vs.* necrosis). To further assess whether the developed method was capable of detecting hepatoprotection, the effect of the known hepatoprotectant, *N*-acetylcysteine, was determined.

Viability decreased in a dose-dependent manner yielding IC₅₀ values of 54 μ M, 64 μ M and 44 μ M for DDT, DDE and DDD, respectively. Evaluation of phase I metabolism showed that



cytochrome P4501A1 activity was dose-dependently induced. Test compounds decreased levels of reactive oxygen species, and significantly hyperpolarised the mitochondrial membrane potential. Assessment of the mode of cell death revealed a significant elevation of caspase-3 activity, with DDD proving to be most potent. DDT alone induced dose-dependent loss of membrane integrity.

These results suggest that the tested compounds produce apoptotic death likely due to mitochondrial toxicity with subsequent caspase-3 activation and apoptotic cell death. The developed *in vitro* assay method reduces the time it would take to assess the tested parameters separately, produces results from multiple endpoints that broadens the scope of toxicity compared to single-endpoint methods. In addition to this the method provides results that are truly comparable as all of the assays utilise the same batch of cells and are conducted on the same plate under the exact same conditions, which eliminates a considerable amount of variability that would be unavoidable otherwise. The present study laid a solid foundation for further development of this method by highlighting the unforeseen shortcomings that can be adjusted to improve scalability and predictive power.

Keywords: Apoptosis, CYP1A1, DDD, DDE, DDT, hepatotoxicity, mechanistic profiling, mitochondrial hyperpolarisation, necrosis, organochlorine, reactive oxygen species.



Table of Contents

List of A	bbre	viations	v
List of Fi	gure	S	viii
List of Ta	ables		χV
Chapter	1: Li	terature review	1
1.1.	Intr	oduction	1
1.2.	Safe	ety evaluation	2
1.3.	The	burden of hepatotoxicity on the pharmaceutical industry	4
1.4.	Нер	atotoxicity	5
1.5.	Mol	ecular mechanisms of hepatotoxicity	6
1.5	.1.	Metabolic activation	7
1.5	.2.	Mitochondrial toxicity	9
1.5	.3.	Oxidative stress	10
1.6.	Nee	ed for improved cell-based hepatotoxicity screening	13
1.7.	Mod	del hepatotoxindel	14
1.8.	Нер	atoprotective agent	16
1.9.	Res	earch topic	17
1.10.	A	ims of the study	18
1.11.	St	tudy objectives	18
Chapter	2: In	Vitro Procedure	19
2.1.	Intr	oduction	19
2.1	.1.	Background	19
2.1	.2.	Hepatotoxic endpoints	20
2.1	.3.	Scope of toxicity	
2.2.	Met	thods	
2.2	.1.	Propagation of Cells	23



2.2	.2.	Cell harvest	3
2.2	.3.	Cell counting	3
2.2	.4.	Microplate setup24	4
2.2	.5.	Test staggering24	4
Chapter	3: In	Vitro Cytotoxicity29	9
3.1.	Bac	kground2	9
3.2.	Met	thods30	0
3.2	.1.	Experimental design	0
3.2	.2.	Viability assay3	1
3.2	.3.	Statistical analyses	1
3.3.	Res	ults3	2
3.4.	Disc	cussion3	8
Chapter	4: Pł	nase I metabolism4	2
4.1.	Bac	kground4	2
4.2.	Met	thods4	4
4.2	.1.	Experimental design4	4
4.2	.2.	Statistical analyses4	5
4.3.	Res	ults4	6
4.3	.1.	Optimisation4	6
4.3	.2.	CYP1A1 induction4	9
4.4.	Disc	cussion5	6
4.4	.1.	Optimisation5	6
4.4	.2.	CYP1A1 activity5	7
Chapter	5: O	xidative Stress6	1
5.1.	Bac	kground6	1
5.2.	Met	thods6	3



	5.2	.1.	Detection of intracellular ROS by fluorometery	.63
	5.2	.2.	Detection of intracellular ROS by flow cytometry	.63
	5.2	.3.	Kinetic evaluation of ROS detected by fluorometry	.64
	5.2	.4.	Statistical analyses	.64
5	5.3.	Res	ults	.65
	5.3	.1.	Endpoint fluorometry	.65
	5.3	.2.	Flow cytometry	.68
	5.3	.3.	Kinetic fluorometry	.69
5	5.4.	Disc	cussion	.73
Cha	apter	6: M	litochondrial Toxicity	.76
6	5.1.	Bac	kground	.76
6	5.2.	Met	thods	.78
	6.2	.1.	Evaluation of $\Delta \psi_{\text{m}}$ using JC-1	.78
	6.2	.2.	Statistical analyses	.79
6	5.3.	Res	ults	.79
6	5.4.	Disc	cussion	.85
Cha	pter	7: M	lodes of Cell Death	.89
7	7.1.	Bac	kground	.89
7	7.2.	Met	thods	.91
	7.2	.1.	Assessment of cell death by apoptosis	.91
	7.2	.2.	Assessment of cell death by necrosis	.91
	7.2	.3.	Statistical analyses	.92
7	7.3.	Res	ults	.92
	7.3	.1.	Assessment of cell death by apoptosis	.92
	7.3	.2.	Assessment of cell death by necrosis	.97
7	7.4.	Disc	cussion	102



Chapte	r 8: Concluding discussion	106
8.1.	Procedure summary	106
8.2.	Test compound mechanism of toxicity	107
8.3.	Advantages of the <i>in vitro</i> model	111
8.4.	Further development of the <i>in vitro</i> model	113
8.5.	In conclusion	115
Annexu	re A: Ethical approval	116
Annexu	re B: Reagents	117
Annexu	re C: Research outputs	121
References		



List of Abbreviations

% percentage degrees Celsius

O₂ superoxide
 OH hydroxyl radical
 7-ER 7-ethoxyresorufin

AAPH 2',2'-azobis(2-methylpropionamidine) dihydrochloride Ac-DEVD-AMC Acetyl-Asp-Glu-Val-Asp-7-amino-4-methylcoumarin

ADP adenosine diphosphate
AhR aryl hydrocarbon receptor

AIDS acquired immune deficiency disease

AMC 7-amino-4-methylcoumarin

Apaf-1 apoptotic protease activating factor-1

Arnt aryl hydrocarbon receptor nuclear translocator

ATP adenosine triphosphate

Bad Bcl-2 associated death promoter

Bax Bcl-2 associated X protein
Bcl-2 B-cell lymphoma 2 protein
BH3 Bcl-2 homology domain 3

Bid BH3 interacting-domain death agonist

Ca²⁺ calcium
Cas-3 caspase 3
CAT catalase

CHAPS 3-[(3-Cholamidopropyl)dimethylammonio]-1-propanesulfonate

 $\begin{array}{ccc} \text{cm} & \text{centimeter} \\ \text{CO}_2 & \text{carbon dioxide} \\ \text{Cu}^{2+} & \text{copper(II)} \\ \text{Cu}^{3+} & \text{copper(III)} \end{array}$

CYP cytochrome P450 cyt C cytochrome C

d days

DCFDA 2'7'-dchlorofluorescein diacetate
DDA bis(p-chlorophenyl)acetic acid
DDD dichlorodiphenyl dichloroethane
DDE dichlorodiphenyl dichloroethylene
DDT dichlorodiphenyl trichloroethane
DISC death-inducing signalling complex

DMSO dimethylsulfoxide
DNA deoxyribonucleic acid

 $\Delta \psi_{\text{m}}$ mitochondrial membrane potential



EDTA ethylenediaminetetraacetic acid
EMEA European Medicines Agency

EMEM Eagle's minimum essential medium ethoxyresorufin-O-deethylase

FADH₂ flavin adenine dinucleotide (reduced)

FCS foetal calf serum

 Fe^{2+} iron(II) Fe^{3+} iron(III) g gram g gravity

G-6-PD glucose-6-phosphate dehydrogenase

GR glutathione reductase

GSH glutathione

GSH-Px glutathione peroxidase gSSG glutathione disulfide

 $\begin{array}{ccc} h & & hour \\ H^{^+} & & proton \\ H_2O & & water \end{array}$

H₂O₂ hydrogen peroxide

HEPES 2-[4-(2-hydroxyethyl)piperazin-1-yl]ethanesulfonic acid

HIV human immunodeficiency virus

HSP90 heat shock protein 90

IC₅₀ concentration at which 50% of cells are not viable

JC-1 5,5',6,6'-tetrachloro-1,1',3,3'- tetraethylbenzimidazolylcarbocyanine iodide

KH₂PO₄ potassium dihydrogen orthophosphate

l litre

LD₅₀ dose at which 50% of the population does not survive

LDH lactate dehydrogenase

M molar milli-

MEIC Multicentre evaluation of *in vitro* cytotoxicity program

Mg²⁺ magnesium (II)

min minutes

MMO microsomal monooxygenase system

mPTP mitochondrial permeability transition pore

mRNA messenger ribonucleic acid

MTT 3-(4,5-Dimethylthiazol-2-yl)-2,5-diphenyltetrazolium bromide

n sample size Na⁺ sodium

NAC *N*-acetylcysteine

NADH nicotinamide adenosine dinucleotide (reduced)

NADPH nicotinamide adenosine dinucleotide phosphate (reduced)

NFI nuclear factor I



NRU neutral red uptake

O₂ oxygen
OH⁻ hydroxyl
p probability

p53 tumour protein 53

PBS phosphate buffered saline

pH negative logarithm of the hydrogen ion concentration

PI propidium iodide ppm parts per million

Puma p53 up-regulated modulator of apoptosis

r² coefficient of determination RFI relative fluorescence intensity

RLW relative liver weight
RNS reactive nitrogen species
ROS reactive oxygen species
RSA Republic of South Africa
SEM standard error of the mean

SOD superoxide dismutase

t test statistic

TCDD 2,3,7,8-tetrachlorodibenzo-*p*-dioxin

U units

UK United Kingdom

US\$ US dollars

USA United States of America

v volume V volts w weight

XRE xenobiotic response element

β beta

γ-GCS γ-glutamylcysteine synthase

 λ_{em} emission wavelength λ_{ex} excitation wavelength

μ micro



List of Figures

Figure 1.1. 8 The relationship between drug metabolism and toxicity. Toxicity may occur through accumulation of parent drug or via metabolic activation, through formation of a chemically reactive metabolite, which, if not detoxified, can effect covalent modification of biological macromolecules. The identity of the target macromolecule and the functional consequence of its modification will dictate the resulting toxicological response. Figure 1.2._____ 12 Cooperation between various antioxidant enzymes and cofactors. SOD – superoxide dismutase, CAT - catalase, GSH - glutathione, GSSG - glutathione disulfide, GSH-Px - glutathione peroxidase, GR glutathione reductase, γ-GCS – γ-glutamylcysteine synthase, GS – glutamine synthase, G-6-PD – glucose-6-phosphate dehydrogenase. 15 Figure 1.3. Illustration of the two routes of metabolism of DDT to produce either DDE or DDD, showing the structure of each of the test compounds utilised in this study. Figure 2.1. 22

Diagram illustrating the scope of toxicity that the chosen parameters are expected to evaluate. As the concentration of test compound increases one would expect to see different cellular responses in an attempt to restore homeostasis. Initially, cells should respond by trying to eliminate xenobiotics through metabolic inactivation (Phase I metabolism). At higher concentrations ROS generation may occur, originating from either mitochondria or from CYP activity. If the mitochondria are affected, they may release factors that will initiate apoptotic death via caspase-3. On the other hand, excessive ROS may result in deactivating caspase activity and lipid peroxidation, which will lead to cell death by necrosis. The degree of toxicity can then be assessed utilising an assay that enumerates viable cells. EROD - ethoxyresorufin-*O*-deethylase, JC-1 - 5,5',6,6'-tetrachloro-1,1',3,3'-tetraethylbenzimidazolylcarbocyanine iodide, DCFDA - 2'7'-dichlorofluorescein diacetate.



Figure 2.2.____ 26 Diagram illustrating the plate setup. Plates were divided into six duplicate column sets, one for each of the six different assays to be performed and into eight rows, for the blanks, controls and various concentrations of test compound. Only one compound was tested on a single plate. Figure 3.1.___ _33 Histogram density plots of the observed viability data of HepG2 cells exposed to DDT demonstrating the distributions of the collected data. The control group is a good example of a normal distribution. The observations did not always follow a normal distribution, especially in the lower ranges of viability. X-axis represents observed values and Y-axis, the count. 34 Figure 3.2. Histogram density plots of the observed viability data of HepG2 cells exposed to DDE demonstrating the distributions of the collected data. The results do not follow a normal distribution. X-axis represents observed values and Y-axis, the count. Figure 3.3._____ 34 Histogram density plots of the observed viability data of HepG2 cells exposed to DDD demonstrating the distributions of the collected data. Data is non-normal as indicated with distinct multiple peaks instead of a single peak. X-axis represents observed values and Y-axis, the count. 37 Fitted dose-response curves of viability of HepG2 cells after DDT, DDE and DDD treatment (mean ± SEM). Dark green curves represent the test compounds alone and light green curves, cells pretreated with NAC. Curves were obtained by fitting viability results to a four-parameter Hill equation with variable slope and the following constraints: top = 100 and bottom = 0. Graphs are plotted on

semi-logarithmic axes. Dashed horizontal lines represents Y = 50%. # = p < 0.001, treatment with test



compound alone compared to controls. \$ = p < 0.05, \$\$ = p < 0.01, \$\$\$ = p < 0.001, pre-treatment with NAC compared to treatment with test compound alone.

Figure 4.1. 47

Scatterplot of EROD assay optimisation for fluorescence substrate concentration. Following 24 h incubation, after seeding, wells were exposed to different concentrations of 7-ER, ranging from 0.5 - 1000 nM, for 1 h and monitored fluorometrically at λ_{ex} = 520, λ_{em} = 595nm. The green line represents blank wells and the red line wells with untreated cells. The dashed vertical line indicates X = 150 nM and the Y-axis represents relative fluorescence intensity (RFI). Values differed significantly from blanks at all points along the graph with \boldsymbol{p} < 0.01.

Figure 4.2. 48

Boxplot of EROD assay with the addition or absence of the cofactor NADPH. To induced CYP1A1 activity, cells were exposed to 100 μ M omeprazole (except controls) for 24 h before performing the EROD assay. Groups represented on the X-axis were exposed to 0, 100 and 150 nM 7-ER for 1 h and fluorometrically monitored at λ ex = 520, λ em = 595nm. Red boxplots represent wells that received 7-ER only, while green boxplots represent those that received 7-ER as well as 100 nM NADPH. Y-axis represents relative fluorescence intensity (RFI), ** indicates p < 0.001.

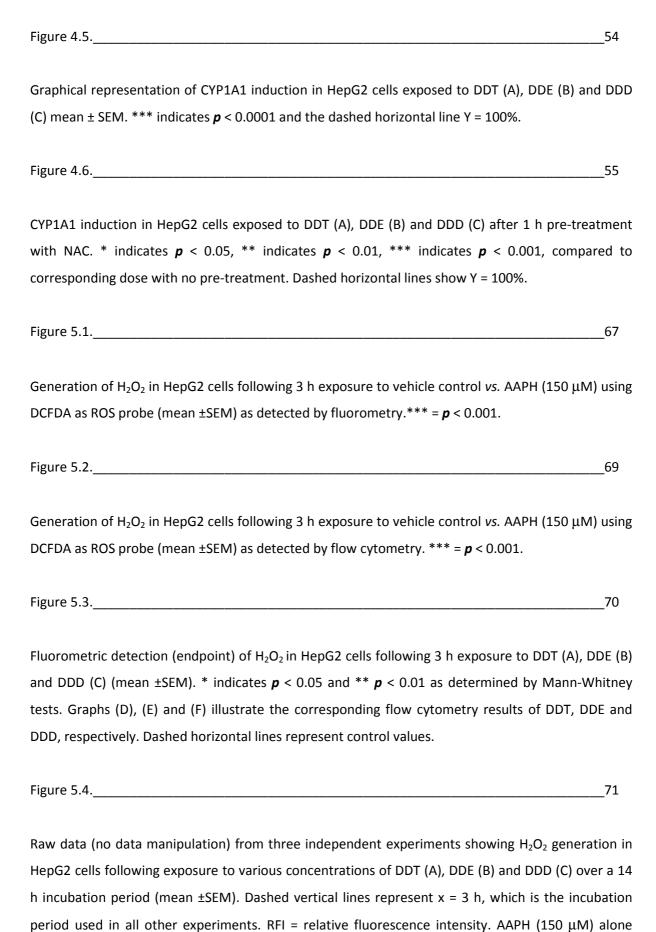
Figure 4.3. 50

Histogram density plots of the observed CYP1A1 data of HepG2 cells exposed to DDT demonstrating the distributions of the collected data, prior to the removal of outliers detected by Grubb's test. The X-axis represents observed values and the Y-axis the count or density.

Figure 4.4. 51

Histogram density plots of the observed CYP1A1 data of HepG2 cells exposed to DDT after the removal of outliers detected by Grubb's test. The X-axis represents observed values and the Y-axis the count or density.







induced significant (p < 0.001) ROS generation from 2 h onwards. All test compounds at all tested concentrations showed no significant difference from the negative control values for the same time.

Generation of H_2O_2 in HepG2 cells following 3 h exposure to DDT, DDE and DDD (mean \pm SEM), with (light green bars) or without (dark green bars) 1 h NAC pre-treatment. No significant differences were detected between the groups.

Figure 6.1._______77

Illustration of the electron transport chain and ATP-synthase embedded in the inner mitochondrial membrane. Electrons enter the system via reduced nicotinamide adenosine dinucleotide (NADH) and reduced flavin adenosine dinucleotide (FADH₂). As electrons are transferred from one respiratory complex to the next, H+ ions are driven from the mitochondrial cytosol into the intermembrane space. O_2 is the final electron receptor, which is reduced to H₂O. ATP-synthase is coupled to this system by the backflow of H+ through the proton channel of ATP-synthase, an ATPase that works in backwards, forming ATP from ADP and inorganic phosphate.

Figure 6.2.______81

Changes in $\Delta\psi_m$ detected by JC-1 in HepG2 cells following 1 h exposure to vehicle control vs. Tamoxifen (150 μ M) (mean ±SEM). Tamoxifen caused significant hyperpolarisation of the membrane potential with p < 0.001 (Student's t-test).

Figure 6.3. 83

Changes in $\Delta \psi_m$ in HepG2 cells following a 1 h exposure to various concentrations of DDT, DDE and DDD (mean \pm SEM) relative to untreated controls. *** = p < 0.001 as determined by Students t-tests and Mann-Whitney tests. Dashed horizontal lines represent Y = 100%.



Figure 6.4. 84

Changes in $\Delta\psi_m$ in HepG2 cells following a 1 h exposure to various concentrations of DDT, DDE and DDD relative to untreated controls. Dark green bars represent cells exposed to test compounds alone and light green bars those with a 1 h pre-treatment with NAC (mean \pm SEM). * = p < 0.05, ** = p < 0.01 and *** = p < 0.001 as determined by Mann-Whitney tests. Dashed horizontal lines represent Y = 100%.

Figure 7.1. 94

Active caspase-3 in HepG2 cells following 6 h exposure to Control vs. Staurosporine (11 μ M) (mean \pm SEM). Staurosporine significantly induced caspase-3 activity with p < 0.001 (***).

Figure 7.2. 96

Caspase-3 activity in HepG2 cells following 6 h exposure to DDT (A), DDE (B) and DDD (C) (mean \pm SEM). Caspase-3 activity was used as a measure of cell death by apoptosis. Graphs (D), (E) and (F) represent the PI staining of cells exposed to DDT, DDE and DDD, respectively. Propidium iodide was used as a measure of membrane integrity and cell death by necrosis. Dashed horizontal lines represent untreated control values. Results are given as mean \pm SEM. ** indicates p < 0.01 and *** p < 0.001 as determined by Mann-Whitney and Student's t-tests, where applicable.

Figure 7.3. 99

Propidium iodide staining as a measure of membrane integrity in HepG2 cells following treatment with 0.5% (v/v) Triton X-100 (TX-100) (mean \pm SEM). *** = p < 0.001.

Figure 7.4. 101

Caspase-3 activity in HepG2 cells following 6 h exposure to DDT (A), DDE (B) and DDD (C) (mean \pm SEM). Graphs (D), (E) and (F) represent the PI staining of cells exposed to DDT, DDE and DDD, respectively. Caspase-3 activity and propidium iodide were used as a measure of cell death by apoptosis and necrosis, respectively. Dashed horizontal lines represent Control values. Results are given as mean \pm SEM. * indicates p < 0.05, ** indicates p < 0.01 and *** p < 0.001 as determined by



Mann-Whitney and Student's *t*-tests, where applicable. Light green bars represent 1 h pre-treatment with NAC as opposed to dark green bars, which received no pre-treatment.

Figure 8.1. 108

Illustration of the three dimensional structure of DDT demonstrating the two aromatic rings, which are not within the same plane.

Figure 8.2.______111

Hypothetical mechanism of the acute toxicity of DDT, DDE and DDD in HepG2 cells after 24 h exposure to 5 - 150 μ M of test compound. At high toxin concentrations (> 50 μ M), the test compounds inhibit ATP synthase either directly or through some unknown mechanism(s). In turn, this elevates $\Delta \psi_m$, resulting in opening of the mPTP and Cyt C release. In the cytosol, Cyt C associates with Apaf-1 and pro-caspase 9 to form the apoptosome, which in turn activates Cas-3, leading to cell death by apoptosis. mPTP = mitochondrial permeability transition pore; Apaf-1 = apoptotic protease activating factor-1; $\Delta \psi_m$ = mitochondrial membrane potential.



List of Tables

Table 2.1. 21
Table 2.121
Parameters of cellular physiology that are suggested by the EMEA and those that were examined in
the present study.
Table 2.225
A summary of the timing followed to perform the six <i>in vitro</i> toxicity assays on a single microplate.
Columns refer to those shown in Figure 2.2.
Table3.135
Shapiro-Francia test results for normality of the observed data. Values given in the table are p-values
and instances where $p < 0.05$ are not normally distributed (*).
Table3.236
IC ₅₀ values (±SEM) of cells with/without NAC pre-treatment prior to test compound exposure.
Table 4.146
Relative fluorescence intensity of resorufin as a result of 7-ER cleavage by untreated HepG2 cells. [7-
ER] = concentration (nM) of substrate employed. Compared to 1 nM, all higher concentrations
yielded significantly different results with $p < 0.05$.
Table 4.248
Effect of the cofactor NADPH on EROD assay results. In Step 2 of optimisation substrate (150 nM),
with or without the addition of 100 nM NADPH was utilised to perform an EROD assay. Results are
presented as mean ± SEM of the relative fluorescence intensity. Statistical analyses of these results
are shown in Figure 4.2.
Table 4.349
Grubb's test results for detecting outliers in the observed CYP1A1 data. Values given in the Table are

 \boldsymbol{p} -values. Instances where \boldsymbol{p} < 0.05 (*) indicates the presence of outliers.



Table 4.451
Shapiro-Francia test results for normality of the observed CYP1A1 data after removal of outliers as detected using Grubb's test. Values given in the Table are p-values. Instances where $p < 0.05$ (*) are significantly non-normal.
Table 4.552
CYP1A1 induction in HepG2 cells following 24 h exposure to DDT, DDE, DDD and the established CYP1A1 inducer, omeprazole (mean \pm SEM). *** indicates p < 0.001 as determined by Mann-Whitney tests.
Table 4.653
CYP1A1 induction in HepG2 cells by DDT, DDE, DDD, with or without 1 h pre-treatment with NAC (mean \pm SEM). *, ** and *** represents \boldsymbol{p} < 0.05, < 0.01 and < 0.001, respectively (Mann-Whitney tests).
Table 5.166
Grubb's test results for detecting outliers in the observed ROS data. Values given in the table are p-values. Instances where $p < 0.05$ (*) indicates the presence of outliers.
Table 5.266
Shapiro-Francia test normality results of the observed ROS data after removal of outliers detected with Grubb's test. Values given in the table are p-values. Instances where $p < 0.05$ are significantly non-normal. * indicates $p < 0.05$.
Table 5.367
ROS generation in HepG2 cells following 3 h exposure to DDT, DDE, DDD and AAPH (positive control). Results (% of Control) are presented as mean \pm SEM. * indicates p < 0.05, ** p < 0.01 and *** p < 0.001 as determined by Mann-Whitney tests.
Table 5.468
ROS generation in HepG2 cells due to DDT, DDE, DDD, with or without 1 h pre-treatment with NAC. There were no statistically significant differences between cells pre-treated with NAC and those that were exposed to test compounds only.



Table 6.1._____ 80 Outliers in $\Delta \psi_m$ data, detected by Grubb's test. Values given in the table are **p**-values. Instances where p < 0.05 (*) indicates the presence of outliers. 80 Table 6.2._____ Shapiro-Francia test normality results of the observed $\Delta\psi_m$ data after removal of outliers detected with Grubb's test. Values given in the table are p-values. Instances where p < 0.05 are significantly non-normal. * indicates p < 0.05. Table 6.3. 81 Changes in $\Delta \psi_m$ in HepG2 cells following 1 h exposure to DDT, DDE, DDD and Tamoxifen (positive control). Results (% of Control) are presented as mean \pm SEM. *** = p < 0.001 as determined by Student's *t*-tests and Mann-Whitney tests. Table 6.4._____ 82 Changes in $\Delta \psi_m$ in HepG2 cells due to DDT, DDE, DDD, with or without 1 h pre-treatment with NAC. * indicates p < 0.05, ** p < 0.01 and *** p < 0.001 as determined by Mann-Whitney tests. Grubb's test results for detecting outliers in Cas-3 data. Values given in the table are p-values. Instances where p < 0.05 (*) indicates the presence of outliers. Table 7.2. 93 Shapiro-Francia test normality results of the observed Cas-3 data after removal of outliers detected with Grubb's test. Values given in the table are p-values. Instances where p < 0.05 are significantly non-normal. * indicates p < 0.05. 94 Table 7.3. Active Cas-3 in HepG2 cells following 6 h exposure to DDT, DDE, DDD and Staurosporine (positive control). Results (% of Control) are presented as mean \pm SEM. ** indicates p < 0.01 and *** p < 0.001as determined by Mann-Whitney and Student's t-tests.



Table 7.4. 97 Relative Cas-3 activity in HepG2 cells after exposure to DDT, DDE, DDD, with or without 1 h pretreatment with NAC. * = \mathbf{p} < 0.05, ** = \mathbf{p} < 0.01, *** = \mathbf{p} < 0.001 as determined by Mann-Whitney and Student's t-tests. Table 7.5._____ 98 Grubb's test results for detecting outliers in the data from PI staining. Values given in the table are pvalues. Instances where p < 0.05 (*) indicates the presence of outliers. Table 7.6. 98 Shapiro-Francia test normality results of the observed PI data after removal of outliers detected with Grubb's test. Values given in the table are p-values. Instances where p < 0.05 are significantly nonnormal. * indicates p < 0.05. 99 Table 7.7._____ PI staining in HepG2 cells following 3 h exposure to DDT, DDE, DDD and Triton X-100 (positive control). Results (% of Control) are presented as mean \pm SEM. * indicates p < 0.05 and ** p < 0.01 as determined by Mann-Whitney tests. Table 7.8._____ 100 PI staining in HepG2 cells due to DDT, DDE, DDD, with or without 1 h pre-treatment with NAC. * indicates p < 0.05 as determined by Mann-Whitney tests.